Understanding and Modeling the Temperature Behavior of Hot-Carrier Degradation in SiON nMOSFETs

Stanislav Tyaginov, Markus Jech, Jacopo Franco, *Member, IEEE*, Prateek Sharma, Ben Kaczer, and Tibor Grasser, *Senior Member, IEEE*

***Abstract*— Using our physics-based model for hot-carrier degradation (HCD), we analyze the temperature behavior of HCD in nMOSFETs with a channel length of 44 nm. It was observed that, contrary to most previous findings, the linear drain current change ($\Delta I_{\mathrm{d,lin}}$) measured during hot-carrier stress in these devices appears to be lower at higher temperatures. However, the difference between the $\Delta I_{\mathrm{d,lin}}$ values obtained at different temperatures decreases as the stress voltage increases. This trend is attributed to the single-carrier process of Si–H bond rupture, which is enhanced by the electron–electron scattering. We also consider another important modeling aspect, namely, the vibrational life-time of the Si–H bond, which also depends on the temperature. We finally show that our HCD model can successfully capture the temperature behavior of HCD with physically reasonable parameters.**

***Index Terms*— Hot-carrier degradation, Si-H bond dissociation, temperature behavior, electron-electron scattering, modeling, interface traps, MOSFET.**

I. Introduction

THE temperature behavior of hot-carrier degradation (HCD) was experimentally shown to change when transistor dimensions scale down. In long-channel devices HCD is suppressed at elevated temperatures [1]–[3], while in short channel devices it typically becomes more severe at higher temperatures [4]–[6]. Summarizing available experimental data one concludes that this transition occurs at channel lengths of around 100 nm.

There are two possibilities for explaining this behavior. The first suggests that the HCD temperature behavior changes at that channel length at which electron-electron scattering (EES) starts to play a dominant role [3], [7]. In fact, EES populates the high-energy tail of the carrier energy distribution function (DF) and thus enhances the defect generation rate [8], [9]. Other scattering mechanisms (scattering at ionized impurities, impact ionization, electron-phonon interactions, etc) lead to a depopulation of the high energy fraction of the carrier ensemble. All these scattering processes have higher rates at elevated temperatures. As a result, in short-channel devices, where EES dominates, HCD is more severe at higher temperatures, while in their longer counterparts HCD is less pronounced because other scattering mechanisms dominate. A modified version of this explanation has been proposed by Bravaix *et al.* [6], who suggest that the temperature behavior of HCD in scaled devices is determined by the multiple-carrier process of Si-H bond rupture. In a later publication of this group [10] the authors suggest that in their devices the role of EES is negligible and thus EES does not determine the temperature behavior of HCD.

The second possible explanation applies to the case of scaled transistors with high-K gate stacks, see [4]. In these devices a contribution provided by the intimately related phenomenon of the negative/positive bias temperature instability (N/PBTI) is strong. As a result, the experimentally observed degradation is a mixture of HCD and BTI. BTI is known to be temperature accelerated, hence the HCD temperature behavior can be contaminated or even overtaken by BTI. For instance, the authors of [4] suggest that even in HfO_2-based transistors with a gate length of 70 nm "pure" HCD appears to be less severe at elevated temperature (T), however, due to the strong opposite dependence of PBTI on temperature, the experimental change increases with T. The imec group also reported the dominating impact of BTI on the temperature behavior of the mixture of BTI and HCD in the case of $HfSiON/SiO_2$ transistors with a channel length of 70 nm, see [5], [11].

These two competing explanations of the HCD temperature behavior already suggest that this behavior depends not only on the gate length but also on the device architecture, gate insulator material and its quality, in addition to the applied stress conditions. In this context - it is quite intriguing - that our measurements have directly shown that even in nMOSFETs with a gate length of 65 nm the change of the linear drain current $\Delta I_{\mathrm{d,lin}}(t)$ recorded during hot-carrier stress is lower at higher temperature. The difference between $\Delta I_{\mathrm{d,lin}}(t)$ values obtained at 25 and 75°C decreases as the

Manuscript received November 11, 2015; accepted November 17, 2015. Date of publication November 25, 2015; date of current version December 24, 2015. This work was supported in part by the Austrian Science Fund (FWF) under Grant P23598 and Grant P26382 and in part by the European Community FP7 projects N$^{\mathrm{o}}$ 619234 (MoRV) and 619246 (ATHENIS 3D). The review of this letter was arranged by Editor X. Zhou.

S. Tyaginov is with the Institute for Microelectronics, Technische Universität Wien, Vienna 1040, Austria, and also with the Ioffe Physical-Technical Institute, Russian Academy of Sciences, Saint Petersburg 194021, Russia (e-mail: tyaginov@iue.tuwien.ac.at).

M. Jech, P. Sharma, and T. Grasser are with the Institute for Microelectronics, Technische Universität Wien, Vienna 1040, Austria.

J. Franco and B. Kaczer are with imec, Leuven 3001, Belgium.

Color versions of one or more of the figures in this letter are available online at http://ieeexplore.ieee.org.

Digital Object Identifier 10.1109/LED.2015.2503920

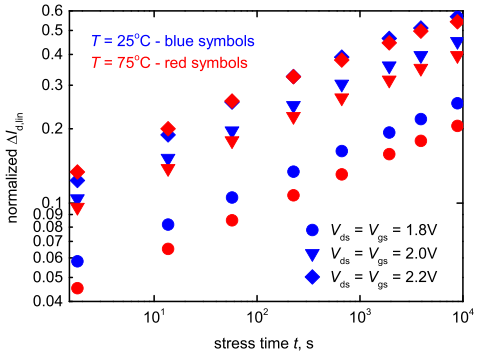

Fig. 1. The change of the linear drain current (normalized to the drain current in the pristine nMOSFET) measured at temperatures of 25 and 75°C. Stress voltages are $V_{ds} = V_{gs} = 1.8$, 2.0, and 2.2 V.

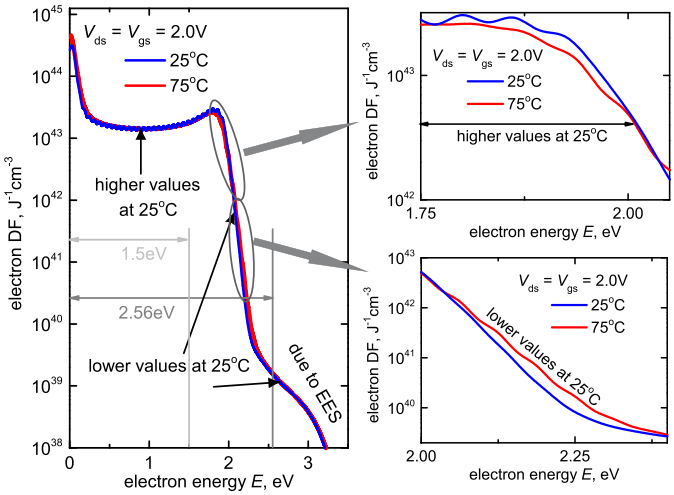

Fig. 2. The near-drain electron DFs simulated with ViennaSHE for $V_{ds} = V_{gs} = 2.0$ V and $T = 25$ and 75°C considering electron-electron scattering. One can see that at lower and moderate energies the DF values are higher at 25°C, while for higher energies the situation is reversed. The pronounced humps in high-energy tails of the DFs are due to electron-electron scattering.

stress voltage grows. We apply our HCD model to explain this unusual temperature behavior of HCD. This study should provide better understanding of the defect generation kinetics and the importance of the single-carrier mechanism of bond dissociation as well as that of EES.

II. Experiment

SiON nMOSFETs with an effective channel length of 44 nm were subjected to hot-carrier stress under $V_{ds} = V_{gs} = 1.8$, 2.0, and 2.2 V and at two different temperatures, i.e. $T = 25$ and 75°C. To asses HCD, $\Delta I_{d,lin}(t)$ traces were recorded up to ~9 ks, Fig. 1. One can see that for $V_{ds} = V_{gs} = 1.8$ and 2.0 V, $\Delta I_{d,lin}$ values for $T = 25$°C are higher than those for $T = 75$°C. This result contradicts previous findings obtained in transistors with comparable gate lengths (e.g. [5] and [6]). Also, the distance between $\Delta I_{d,lin}(t)$ curves reduces as V_{ds}, V_{gs} increase, and at $V_{ds} = V_{gs} = 2.2$ V the $\Delta I_{d,lin}$ values are almost the same for both T within the whole stress time slot. Note that – in order to exclude possible measurement artefacts and acquire reliable HCD data – for each degradation curve four samples were used. $\Delta I_{d,lin}(t)$ traces showed good repeatability and sample-to-sample variations were negligibly small.

Special attention must be paid to guarantee that device degradation is caused by HCD, rather than by a mixture of HCD and PBTI. This issue has already been addressed in our previous paper which dealt with the same devices [8]. First, samples stressed at both temperatures and different V_{ds}, V_{gs} values showed no recovery. Second, the charge-pumping signal plotted as a function of the varying high level voltage did not reveal a plateau. This excludes possible contribution of bulk oxide traps to the damage and makes the effect of PBTI negligibly small.

III. Dissociation Energetics of the Si-H Bond

We assume that HCD is driven by the generation of interface traps due to the dissociation of pristine Si-H bonds at the interface. The Si-H bond is described within the truncated harmonic oscillator model [8], [9]. Bond rupture is modeled as a superposition of the multiple vibrational excitation (MVE-process) of the bond by carriers with total energy

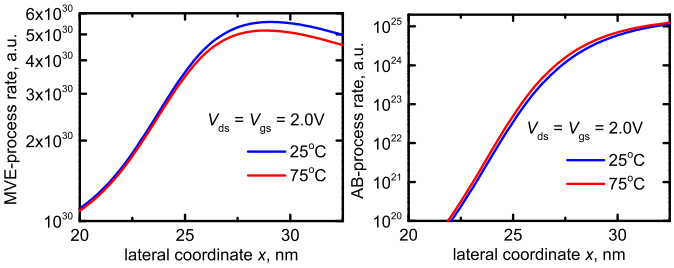

Fig. 3. The rates of the MVE- and AB-processes simulated for two different temperatures of 25 and 75°C for the drain side.

smaller than the bond-breakage activation energy E_a and hydrogen release from any of the oscillator levels (AB-process) [8], [9]. In previous HCD models [12]–[14], the bond heating terminated by hydrogen hopping from the last bonded state to the transport mode was referred to as the multiple-carrier process, while a direct H desorption from the ground state by a solitary hot carrier was referred to as the single-carrier process.

The rates of the MVE- and AB-processes are described by the carrier acceleration integral: $I^{AB/MVE} = \int f(E)g(E)v(E)\sigma^{AB/MVE}(E)dE$, where f is the DF, g the density-of-states, v the group velocity, $\sigma^{AB/MVE}(E)$ the reaction cross sections for AB- and MVE-mechanisms, while E is the carrier energy. The carrier DFs are obtained using the deterministic Boltzmann transport equation solver ViennaSHE [8], [9], while the reaction cross section is modeled as $\sigma^{AB/MVE} = \sigma_0^{AB/MVE} \times (E - E_{th}^{AB/MVE})^p$. For the MVE-process the threshold energy is equal to the distance between the oscillator levels $\hbar\omega$. Another parameter that determines the bond energetics is the depth of the oscillator quantum well, i.e. the bond-breakage energy E_a. This parameter also determines the height of the potential barrier separating the bond level i (with the energetical

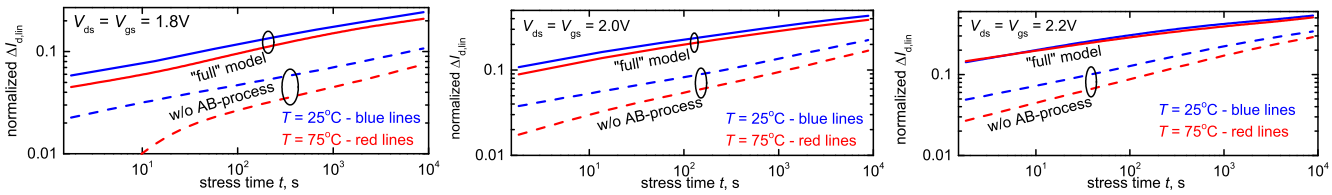

Fig. 4. The $\Delta I_{\mathrm{d,lin}}(t)$ curves evaluated with the "full" model and neglecting the AB-process. The distance between the $\Delta I_{\mathrm{d,lin}}(t)$ curves obtained for $T = 25$ and 75°C increases if the AB-mechanism is not considered.

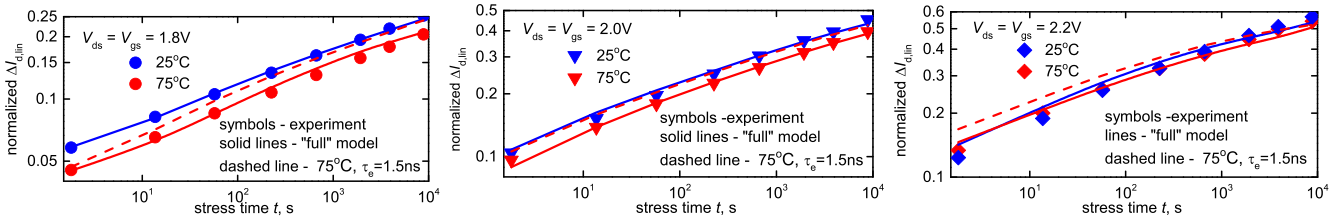

Fig. 5. The $\Delta I_{\mathrm{d,lin}}(t)$ traces for three different combinations of stress voltages $V_{\mathrm{ds}} = V_{\mathrm{gs}} = 1.8\,\mathrm{V}$, $V_{\mathrm{ds}} = V_{\mathrm{gs}} = 2.0\,\mathrm{V}$, and $V_{\mathrm{ds}} = V_{\mathrm{gs}} = 2.2\,\mathrm{V}$ and two temperatures, i.e. 25 and 75°C. We also simulated the $\Delta I_{\mathrm{d,lin}}(t)$ traces for $T = 75$°C but using the same value of the vibrational life-time $\tau_{\mathrm{e}} = 1.5\,\mathrm{ns}$ as for 25°C (represented by dashed lines). The agreement between experimental data and model results is very good.

position E_i) and the transport mode: $E_{\mathrm{a}} - E_i - d \times F_{\mathrm{ox}}$, where d is the bond dipole moment and F_{ox} is the oxide electric field [8], [9], [13].

There are two vibrational modes of the Si-H bond, namely stretching (with $\hbar\omega = 0.25\,\mathrm{eV}$ and $E_{\mathrm{a}} = 2.5\,\mathrm{eV}$) and bending ($\hbar\omega = 0.075\,\mathrm{eV}$ and $E_{\mathrm{a}} = 1.5\,\mathrm{eV}$) [13], [15]. In one of the most successful HCD models developed by the Bravaix group it is assumed that bond dissociation occurs via the bending mode with the corresponding values of $\hbar\omega$ and E_{a} [13]. The vibrational life-time (τ_{e}) chosen in that model is 10 ps and – to the best of our knowledge – its temperature dependence is not considered [6], [13]. Experimental investigations, however, suggest that H desorption from the Si/SiO_2 interface occurs with $E_{\mathrm{a}} = 2.56\,\mathrm{eV}$ [16], [17]. This value is close to that typical for the stretching mode with the corresponding vibrational life-times at $T = 25$ and 75°C of 1.5 and 1.3 ns, respectively, see [18]. These parameter values are used in our HCD model.

IV. Results and Discussion

An example of the electron DF simulated for $V_{\mathrm{ds}} = V_{\mathrm{gs}} = 2.0\,\mathrm{V}$ and two different temperatures is presented in Fig. 2. One can see that for low and moderate energies (at the phonon cascade plateau) the DF values are higher at 25°C, while high-energy tails are more populated at 75°C (e.g. the EES induced hump). Such a behavior allows us to conclude that the MVE-process rate should be higher at 25°C, while the AB-process rate increases with temperature. This is confirmed by Fig. 3 where the corresponding rates are depicted for the same conditions. Note that these rates vary by many orders of magnitude, and thus are plotted only for the near-drain transistor fragment in order to better depict the temperature effect. Another factor which determines the impact of temperature on the MVE-process kinetics is the vibrational life-time which decreases with T: at higher temperatures the vibrational levels depopulate faster and a higher carrier flux is needed to maintain the bond-breakage rate at the same level.

Thus, for a proper model calibration one needs to choose the capture cross section values for the MVE- and AB-processes to ensure domination of the former mechanism with the latter one still having a pronounced rate. At higher voltages $V_{\mathrm{ds}} = V_{\mathrm{gs}} = 2.2\,\mathrm{V}$ the AB-process should become dominant, thereby controlling the temperature behavior of HCD and leading to the same $\Delta I_{\mathrm{d,lin}}$ values for both T. Such a tendency was obtained with the capture cross sections of $\sigma_0^{\mathrm{AB}} = 5\times10^{-18}\,\mathrm{cm}^{-2}$ and $\sigma_0^{\mathrm{MVE}} = 5\times10^{-19}\,\mathrm{cm}^{-2}$. It is worth to comment that in the previous version of our model, as well as in the Bravaix approach, [8], [9] the bond-breakage energy was chosen to be 1.5 eV. Although our model was able to represent experimental data, a physically unreasonable low value $\sigma_0^{\mathrm{AB}} = 2.5\times10^{-23}\,\mathrm{cm}^{-2}$ was used. In addition, $E_{\mathrm{a}} = 1.5\,\mathrm{eV}$ contradicts the experimental observations [16], [17]. Fig. 4 summarizes degradation traces simulated with the "full" version of our new model and neglecting the AB-process. We can see that the distance between the $\Delta I_{\mathrm{d,lin}}(t)$ curves obtained for the two temperatures substantially increases when the AB-process is neglected.

Note finally that HCD itself is a very complex phenomenon which cannot be described by a single process. For a proper description, which is valid for different technologies, the interplay between various mechanisms needs to be considered. As we have shown in [8], [19], and [20] even in long-channel and/or high-voltage devices one cannot neglect the contribution of electron-electron scattering and the multiple-carrier process of bond dissociation. On the other hand, the single-carrier mechanism plays a significant role also in decananometer devices [8]. The same holds true for the intricate temperature behavior of HCD. Only after all the effects are taken into account, combined with the temperature dependent vibrational life-time, the true temperature characteristic of HCD can be revealed.

Finally, we would like to emphasize that Fig. 5 shows very good agreement between experimental data and the model results.

V. Conclusions

Measurements of the linear drain current change during hot-carrier stress in an nMOSFET with an effective channel length of 44 nm have revealed that at lower stress voltages the degradation becomes less severe at elevated temperature, while at higher V_{ds}, V_{gs}, the $\Delta I_{d,lin}$ values are the same. This behavior was explained by considering two coupled mechanisms responsible for Si-H bond-breakage: bond excitation by cold carriers and hydrogen release triggered by a solitary carrier. The rate of the former process was shown to decreases with temperature, while the latter process becomes more important (note that EES enhances the AB-process rate). The vibrational lifetime – a crucial component in modeling HCD – reduces with temperature, thereby also affecting the bond-breakage rate. Our HCD model was able to represent experimental data using a set of physically reasonable parameters. For instance, the bond-breakage energy should be 2.56 eV in agreement with experimental findings. Note finally that the HCD temperature behavior is determined by the interplay of the device geometry with the stress/operating conditions, rather than by the channel length alone.

References

[1] F.-C. Hsu and K. Y. Chiu, "Temperature dependence of hot-electron-induced degradation in MOSFET's," *IEEE Electron Device Lett.*, vol. 5, no. 5, pp. 148–150, May 1984. DOI: 10.1109/EDL.1984.25865

[2] M. Song, K. P. MacWilliams, and J. C. S. Woo, "Comparison of NMOS and PMOS hot carrier effects from 300 to 77 K," *IEEE Trans. Electron Devices*, vol. 44, no. 2, pp. 268–276, Feb. 1997. doi: 10.1109/16.557714

[3] Z. Song, Z. Chen, A. Z. Yong, Y. Song, J. Wu, and K. Chien, "The failure mechanism worst stress condition for hot carrier injection of NMOS," *ECS Trans.*, vol. 52, no. 1, pp. 947–952, 2013. DOI: 10.1109/16.557714

[4] K. T. Lee, C. Y. Kang, O. S. Yoo, R. Choi, B. H. Lee, J. C. Lee, H.-D. Lee, and Y.-H. Jeong, "PBTI-associated high-temperature hot carrier degradation of nMOSFETs with metal-gate/high-*k* dielectrics," *IEEE Electron Device Lett.*, vol. 29, no. 4, pp. 389–391, Apr. 2008. DOI: 10.1109/LED.2008.918257

[5] E. Amat, T. Kauerauf, R. Degraeve, R. Rodríguez, M. Nafría, X. Aymerich, and G. Groeseneken, "Channel hot-carrier degradation in pMOS and nMOS short channel transistors with high-*k* dielectric stack," *Microelectron. Eng.*, vol. 87, no. 1, pp. 47–50, 2010. DOI: 10.1016/j.mee.2009.05.013

[6] A. Bravaix, V. Huard, D. Goguenheim, and E. Vincent, "Hot-carrier to cold-carrier device lifetime modeling with temperature for low power 40 nm Si-bulk NMOS and PMOS FETs," in *Proc. IEEE Int. Electron Devices Meeting (IEDM)*, Dec. 2011, pp. 27.5.1–27.5.4. DOI: 10.1109/IEDM.2011.6131625

[7] S. E. Rauch, F. J. Guarin, and G. LaRosa, "Impact of E-E scattering to the hot carrier degradation of deep submicron NMOSFETs," *IEEE Electron Device Lett.*, vol. 19, no. 12, pp. 463–465, Dec. 1998. DOI: 10.1109/55.735747

[8] M. Bina, S. Tyaginov, J. Franco, K. Rupp, Y. Wimmer, D. Osintsev, B. Kaczer, and T. Grasser, "Predictive hot-carrier modeling of n-channel MOSFETs," *IEEE Trans. Electron Devices*, vol. 61, no. 9, pp. 3103–3110, Sep. 2014. DOI: 10.1109/TED.2014.2340575

[9] S. Tyaginov, M. Bina, J. Franco, D. Osintsev, O. Triebl, B. Kaczer, and T. Grasser, "Physical modeling of hot-carrier degradation for short- and long-channel MOSFETs," in *Proc. IEEE Int. Rel. Phys. Symp. (IRPS)*, Jun. 2014, p. XT.16-1–XT.16–8. DOI: 10.1109/IRPS.2014.6861193

[10] Y. M. Randriamihaja, X. Federspiel, V. Huard, A. Bravaix, and P. Palestri, "New hot carrier degradation modeling reconsidering the role of EES in ultra short N-channel MOSFETs," in *Proc. IEEE Int. Rel. Phys. Symp. (IRPS)*, Apr. 2013, pp. XT.1.1–XT.1.5. DOI: 10.1109/IRPS.2013.6532116

[11] E. Amat, T. Kauerauf, R. Rodriguez, M. Nafria, X. Aymerich, R. Degraeve, and G. Groeseneken, "A comprehensive study of channel hot-carrier degradation in short channel MOSFETs with high-*k* dielectrics," *Microelectron. Eng.*, vol. 103, no. 3, pp. 144–149, 2013. DOI: 10.1016/j.mee.2012.10.011

[12] W. McMahon, K. Matsuda, J. Lee, K. Hess, and J. Lyding, "The effect of a multiple carrier model of interface trap generation on lifetime extraction for MOSFETs," in *Proc. Int. Conf. Modeling Simulation Microsyst.*, vol. 1. 2002, pp. 576–579.

[13] C. Guerin, V. Huard, and A. Bravaix, "General framework about defect creation at the Si/SiO_2 interface," *J. Appl. Phys.*, vol. 105, no. 11, pp. 114513-1–114513-12, 2009. DOI: 10.1063/1.3133096

[14] S. E. Tyaginov, I. A. Starkov, O. Triebl, J. Cervenka, C. Jungemann, S. Carniello, J. M. Park, H. Enichlmair, C. Kernstock, M. Karner, E. Seebacher, R. Minixhofer, H. Ceric, and T. Grasser, "Interface traps density-of-states as a vital component for hot-carrier degradation modeling," *Microelectron. Rel.*, vol. 50, nos. 9–11, pp. 1267–1272, 2010. DOI: 10.1063/1.3133096

[15] B. N. J. Persson and P. Avouris, "Local bond breaking via STM-induced excitations: The role of temperature," *Surf. Sci.*, vol. 390, nos. 1–3, pp. 45–54, 1997. DOI: 10.1016/S0039-6028(97)00507-4

[16] K. L. Brower, "Dissociation kinetics of hydrogen-passivated (111) Si-SiO_2 interface defects," *Phys. Rev. B*, vol. 42, no. 6, pp. 3444–3454, 1990. DOI: 10.1103/PhysRevB.42.3444

[17] A. Stesmans, "Passivation of P_{b0} and P_{b1} interface defects in thermal (100) Si/SiO_2 with molecular hydrogen," *Appl. Phys. Lett.*, vol. 68, no. 15, pp. 2076–2078, 1996. DOI: 10.1063/1.116308

[18] I. Andrianov and P. Saalfrank, "Theoretical study of vibration-phonon coupling of H adsorbed on a Si(100) surface," *J. Chem. Phys.*, vol. 124, no. 3, pp. 034710-1–034710-10, 2006. DOI: 10.1063/1.2161191

[19] S. Tyaginov, M. Bina, J. Franco, Y. Wimmer, B. Kaczer, and T. Grasser, "On the importance of electron–electron scattering for hot-carrier degradation," *Jpn. J. Appl. Phys.*, vol. 54, no. 4S, pp. 04DC18-1–04DC18-6, 2015. DOI: 10.7567/JJAP.54.04DC18

[20] P. Sharma, S. Tyaginov, Y. Wimmer, F. Rudolf, K. Rupp, M. Bina, H. Enichlmair, J.-M. Park, R. Minixhofer, H. Ceric, and T. Grasser, "Modeling of hot-carrier degradation in nLDMOS devices: Different approaches to the solution of the Boltzmann transport equation," *IEEE Trans. Electron Devices*, vol. 62, no. 6, pp. 1811–1818, Jun. 2015. DOI: 10.1109/TED.2015.2421282